

# The effect of fuel sulfur content on the emission characteristics of marine auxiliary diesel engine

Lintao Wei<sup>1</sup>, Bowen Zhao<sup>1</sup>, Song Zhang<sup>1</sup>, Xingyu Liang<sup>1\*</sup>

<sup>1</sup> State Key Laboratory of Engines, Tianjin University, Tianjin 300072, China (Corresponding Author)

## ABSTRACT

With the increasing focus on black carbon emissions in the International Maritime Organization, It is increasingly important to study the influence of fuel sulfur content on marine diesel engine emission, especially on particulate matter emission, a 4.5 L Marine auxiliary engine was tested with different Fuel sulfur content FSC (0.26% , 0.05% and 0.005%), the effects of fuel sulfur content on the Brake Thermal Efficiency (BTE) were analyzed. And then the variations of conventional and unconventional gas emissions with FSC were measured, such as CO, CO<sub>2</sub>, CH<sub>4</sub>, and SO<sub>2</sub>. Then, based on the difference of the FSN and the PN of PM, the effect of PM morphology was discussed. The results show that with the increase of sulfur content, BTE decreases, CO and THC emissions increase, which are due to the more presence of fuel incomplete combustion products. With the increase of FSC, the fractal dimension( $D_f$ ) of particle aggregates increases, the rotational diameter( $D_g$ ) of particle aggregates increases, more particles are tightly bound together in clusters. So that PN decreases, but FSN increases.

**Key words:** Fuel Sulfur Content; marine auxiliary diesel engine.

## 1. INTRODUCTION

The shipping plays a key role in the international transportation because of its better fuel economy. However, shipping emissions is also the main source of air pollution [1]. As it reported, there were 961 Mt (million tons) of CO<sub>2</sub> equivalents, 20.9 Mt of NO<sub>x</sub>, 11.3 Mt of SO<sub>x</sub> and 1.4 Mt of PM (particulate matter) in global total emissions for shipping, which were harmful to human health [2]. In response to increasing emissions, the International Maritime Organization (IMO) introduced much stringent regulations, especially limitations for sulfur, NO<sub>x</sub> and PM emissions [3]. The second phase of marine engine emission legislation in China (China II) introduced more stringent emissions limitation, which will come into force on 1st July 2021. To

meet new regulations, it is necessary to further investigate the shipping emissions [4-5].

The regulated emissions, such as CO, HC, NO<sub>x</sub> and PM, are mainly influenced by fuel compositions, such as sulfur content. Tan et al. [6] reported that fuel sulfur contents had obvious impacts on smoke emissions, but not significant for NO<sub>x</sub>. In addition, they [7] found that sulfur also had an effect on the structure and physico-chemical properties of particulate matter produced by the engine after testing the engine with lubricants with different sulfur content. Van et al. [8] suggested that with FSC increased, the combustion became worse under all load conditions, as well as more particle number and mass. Zhao et al. [9] studied the properties of particulate matter in Lean and Rich Flames in a co-flow combustor using fuels with different FSC, it is found that sulfur has some effect on the evolution and growth of particulate matter entering the atmosphere.

Nevertheless, there are still lack of systemic investigations on the effects of fuel with different sulfur contents on marine auxiliary diesel engine performance, especially unregulated emissions. In present study, different sulfur content fuels (0.26%, 0.05% and 0.005%) were tested on a 4.5L marine auxiliary diesel engine. The regulated emissions, including CO, CO<sub>2</sub>, NO<sub>x</sub>, THC (total hydrocarbon), FSN (filter smoke number) and PN (particle number), were tested by exhaust gas analyzer (Horiba MEXA-ONE-01-OV). The PN and FSN were tested by AVL 489 and AVL 415, respectively. The unregulated emissions, such as CH<sub>4</sub>, HCHO, HCOOH, C<sub>2</sub>H<sub>4</sub>, N<sub>2</sub>O, SO<sub>2</sub> were analyzed by FTIR. The particulate matter samples were collected by a sampler under various working conditions and observed under transmission electron microscope. The differences of particulate matter emission were analyzed in terms of micro-morphology.

## 2. EXPERIMENTAL METHODOLOGY

### 2.1 Test engine, test conditions and fuel

Marine auxiliary machinery is a kind of power generating equipment widely used on large ocean-going

ships [10]. In this study, a four-cylinder, four-stroke turbocharged marine auxiliary diesel engine is used. The engine parameters are listed in Table 1. The schematic diagram of the test bench is shown in Fig. 1. The engine used in the test is coupled to the eddy current dynamometer and some analysis equipment. Several emissions of interest in this study, such as conventional gas emissions, unconventional gas emissions, and particulate matter emissions, were measured using a combination of several sets of equipment. Conventional emissions of CO, CO<sub>2</sub>, NO<sub>x</sub> and THC are recorded by the HORIBA MEXA-ONE-01-OV. The emission of unconventional pollutants such as CH<sub>4</sub>, HCHO, HCOOH, C<sub>2</sub>H<sub>4</sub>, N<sub>2</sub>O and SO<sub>2</sub> in tail gas was determined by AVL infrared spectroscopy. PN and FSN were detected by AVL 489 and AVL 415 respectively. The particulate matter in the exhaust gas was sampled with a filter sampling system and a copper mesh microgrid.

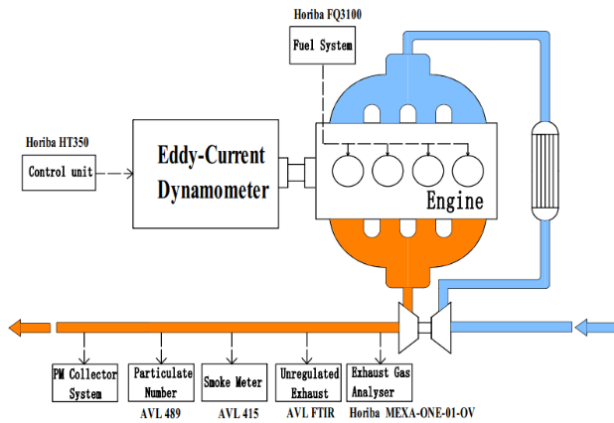


Fig 1. Schematic diagram of experimental setup

In the present study, the engine speed was controlled at 2100 rpm with four engine loads (25%, 50%, 75%, 100%). At each operating condition, the room temperature, cooling water temperature and lubricating oil temperature was controlled at  $20 \pm 3$  °C,  $85 \pm 1$  °C and  $95 \pm 1$  °C, respectively. Sulfur contents were the main parameters of fuel which affected fuel combustion deeply. Meanwhile, deciding proper sulfur contents would be helpful to fit new emission regulations. Three fuels were employed in this work, including S0.005, S0.05, S0.26 (0.005%, 0.05% and 0.26% sulfur contents in fuel). The fuel specifications are presented in Table 3. Lubricant oil Mobil 15w-40 CK-4 was used in this work.

Tab.1 Engine specifications

Categories	Parameters
Number of cylinders	4
Maximum speed	2100 r/min
Itineraries	130 mm

Cylinder diameter	105 mm
Compression ratio	11:1
Number of valves per cylinder	4
Total displacement	4.5 L
Fuel Injection	Engine driven fuel pump

Tab.2 Test conditions

Fuel	Rotational speed (r/min)	Load (%)
S0.005	2100	25%,50%,75%,100%
S0.05	2100	25%,50%,75%,100%
S0.26	2100	25%,50%,75%,100%

Tab.3 Diesel fuel specifications

Nature	S0.005	S0.05	S0.26
Cetane number	48.9	49.1	49.4
Kinematic viscosity (mm <sup>2</sup> /s)	3.625	3.563	3.502
Sulfur content (mg/kg)	53	504	2592
Flash Point (°C)	68	65	61
Freezing Point (°C)	-12	-12	-18
Density (kg/m <sup>3</sup> )	838.9	839.2	840.3

## 2.2 Methods for sampling and analysis of particulate matter

In this system, a sampling branch pipe is used to drain the exhaust gas from the exhaust pipe. The exhaust gas flows through the pipe and the PM is thermally sampled at the outlet with a copper mesh micro-grid. The samples were analyzed using Transmission Electron microscope(TEM). At 25% load, particulate emissions from engines using three different FSC were collected, and the sampling time of all working conditions was 10s in order to ensure that the number of particles attached to the monoxide film that coated with 200 copper grids of TEM was sufficient and did not pile up and overlap, in this way, the observation requirements of TEM can be satisfied.

In this paper, the microstructure and nano-parameters of soot particles were characterized by JEOL2010FEF type HRTEM produced by joint-stock company, Japan. HRTEM image with scale of 50nm was obtained at 40000x magnification.

### 3. RESULTS AND DISCUSSION

#### 3.1 Effect of fuel sulfur content on engine performance

The trend in thermal efficiency (BTE) is shown in Figure 2. Under the condition of low load, the combustion temperature in the cylinder is lower, which further aggravates the incomplete combustion in the cylinder. With the increase of sulfur content in fuel, the combustion efficiency of fuel decreases. In addition, the presence of sulfur in fuel, like carbon, reacts with oxygen during fuel combustion to produce SOx and sulfate. Therefore, if the sulfur content of the fuel is high, it will

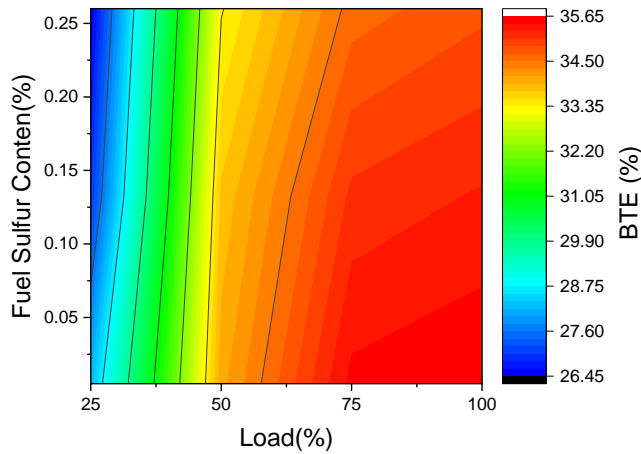


Fig.2 Brake thermal efficiency variation with engine load and fuel sulfur content.

absorb more oxygen during the intake and combustion process, thus ensuring that the fuel burns with enough oxygen [11].

#### 3.2 Effect of FSC on engine emissions

##### 3.2.1 Conventional discharge

The conventional emission test results of the engine are shown in Figure 3, including CO, CO<sub>2</sub>, THC, NO<sub>x</sub>, FSN, and PN emissions as required by the emission regulations. CO and THC emissions were similar with engine load and FSC, but decreased with load and increased with FSC. Both of these pollutants are the products of incomplete combustion in cylinder. Accordingly, CO<sub>2</sub> and NO<sub>x</sub> emissions with the engine load and FSC changes in the cloud graph distribution and the former two trends in the opposite direction, higher emissions in the region (the red part of the map) concentrated in the high-load region. Especially at full load, there is a trough of NO<sub>x</sub> emissions with the increase of sulfur content in the fuel. First of all, it can be seen in table 3 that the fuel of S0.26 has a higher cetane number than the fuel of low sulfur, which leads to a higher combustion temperature [12] in the cylinder, sulfur can also combine with oxygen to form gaseous sulfur oxides and sulfates during combustion, which affects the combustion efficiency of fuel and, to some extent, the formation of NO<sub>x</sub>. Therefore, under the combined action of these two factors, the NO<sub>x</sub> emission decreases first and then increases with the change of sulfur content.

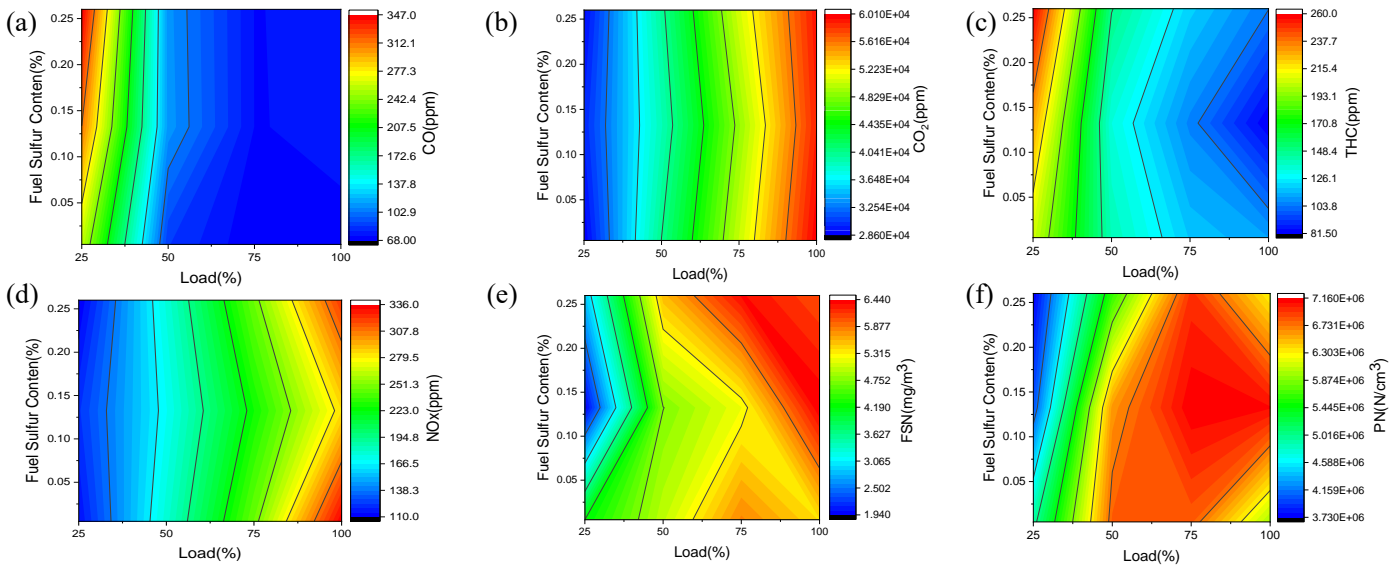


Fig 3. (a) CO, (b) CO<sub>2</sub>, (c) THC, (d) NO<sub>x</sub>, (e) FSN and (f) PN, as functions of engine loads and FSC

### 3.2.2 Unregulated emissions

Emissions of  $\text{CH}_4$ ,  $\text{C}_2\text{H}_4$ ,  $\text{HCOOH}$ ,  $\text{HCHO}$ ,  $\text{SO}_2$  and  $\text{N}_2\text{O}$  from fuels with different FSC are shown in Figure 4.  $\text{CH}_4$  is the smallest hydrocarbon, it is a kind of saturated hydrocarbon emissions, mainly from the fuel cracking, reforming and polymerization of three processes. Methyl groups ( $\text{CH}_3\cdot$ ) and hydrogen atoms ( $\text{H}\cdot$ ) are formed in the process of fuel cracking, and  $\text{CH}_4$  is finally produced through hydrogenation. When engines burn fuels with high sulfur content at low load conditions, more incomplete combustion products are produced and more fuel is cracked [13].  $\text{C}_2\text{H}_4$  is mainly formed by pyrolysis of diesel oil. Ethylene is one of the most important intermediates in the combustion pyrolysis or oxidative pyrolysis of the macromolecular hydrocarbons and macromolecular alkanes in diesel oil. Therefore, its emission characteristics are similar to that of  $\text{CH}_4$ , but  $\text{CH}_4$  is more affected by the sulfur content of the fuel than  $\text{C}_2\text{H}_4$ .

In the cracking process of a macromolecule fuel, the methyl group formed after breaking the bond of the primary carbon atom is an important precursor for the formation of methane, the intermediate secondary carbon atom requires less energy to break a bond, an important difference in the  $\text{CH}_4$  and  $\text{C}_2\text{H}_4$  generation pathways [14]. Therefore, it is possible that sulfur may have an effect on C-C bond fracture during fuel cracking,

and promote the fracture of carbon bond on primary carbon. Both  $\text{HCOOH}$  and  $\text{HCHO}$  are made up of carbonyl groups, double bonds between carbon atoms and oxygen. At the same time, they are the intermediate products produced in the process of combustion and pyrolysis of macromolecular fuels, which mainly come from incomplete combustion [15-16]. Methyl is also an important precursor of  $\text{HCOOH}$ , the higher temperature in the cylinder under high load conditions makes the primary carbon easier to break bonds to form methyl groups, and the high content of sulfur may also promote the formation of methyl groups, therefore,  $\text{HCOOH}$  emissions were higher in the high sulfur content and high load region.  $\text{HCHO}$  is mainly produced by the oxidation reaction of  $\text{C}_2\text{H}_4$ , so it is similar to the distribution of  $\text{C}_2\text{H}_4$ , but the reaction of  $\text{HCHO}$  is restrained under the condition of high equivalent ratio, thus, there is a difference in the area of high load and low sulfur content, as shown in Figure 4 (e),  $\text{SO}_x$  is mainly produced in the combustion process, which is related to the FSC. At the same time, with the increase of load, the air-fuel ratio decreases, and the incomplete sulfur combustion product  $\text{SO}_2$  increases with the increase of sulfur content. Therefore, with the increase of FSC,  $\text{SO}_2$  emissions increase significantly. In contrast,  $\text{N}_2\text{O}$  formation is affected by in-cylinder temperature and oxidation, with high emission red areas concentrated in areas with high FSC and low engine load.

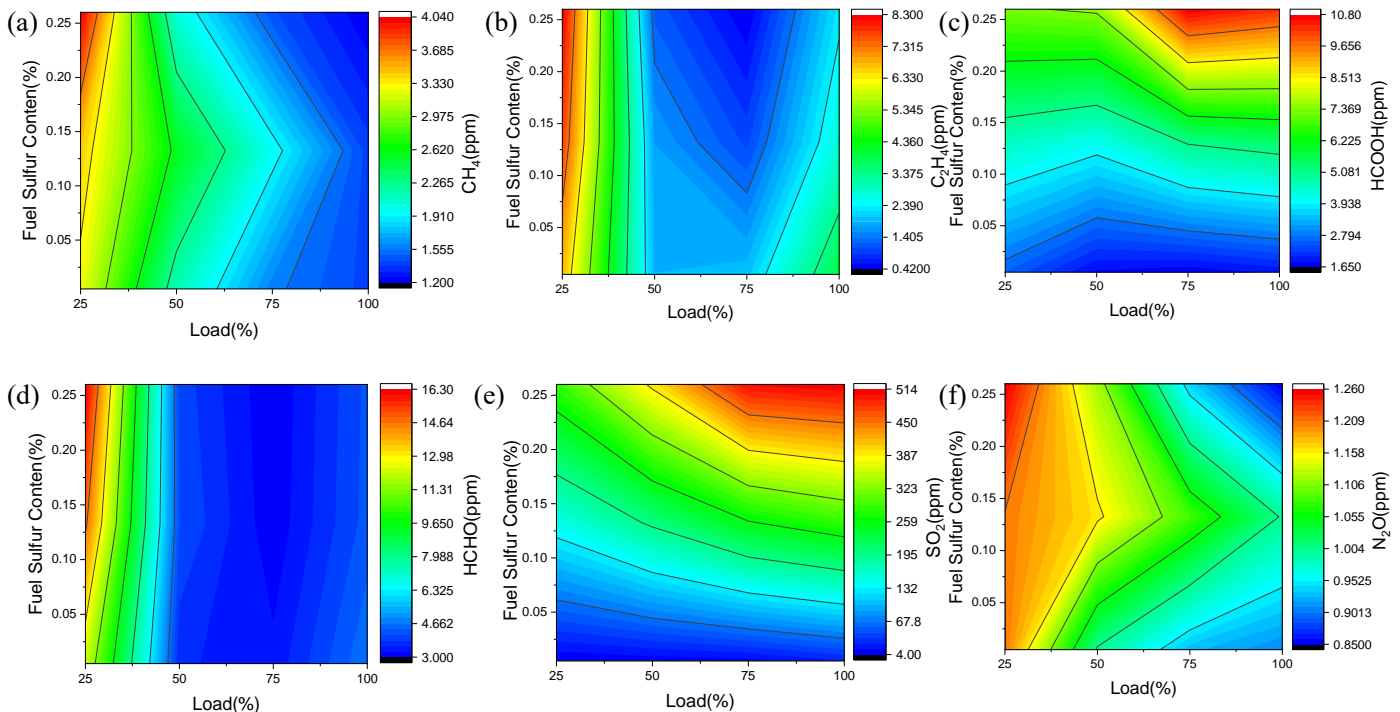


Fig 4. (a)  $\text{CH}_4$ , (b)  $\text{C}_2\text{H}_4$ , (c)  $\text{HCOOH}$ , (d)  $\text{HCHO}$ , (e)  $\text{SO}_2$  and (f)  $\text{N}_2\text{O}$  as functions of engine loads and FSC

### 3.3 Study on emission difference between PN and FSN of particulate matter

As can be seen from Figure 3 (e), (f), the PN values are mainly concentrated in the blue region at 25% load. The trends in FSN and PN are inconsistent, the reason may be that the increase of sulfur leads to the change of particle micro-morphology, especially the change of particle agglomerate shape and size, which leads to the difference of particle FSN and PN.

Aggregates are an intermediate state between the primary particles and the deposited particles of diesel particulate matter. It is formed by agglomeration of primary particles produced during combustion in the cylinder. The primary particles suspended in the combustion chamber are driven by the air-fuel mixture or the exhaust stream and collide with each other continuously, thus accumulating into agglomerates containing multiple particles, and may undergo another collision process to grow into larger aggregates. At the same time, the primary particles still undergo surface growth and oxidation during the aggregation process. The morphology of aggregates is mainly reflected by their fractal dimension ( $D_f$ ).  $D_f$  is a parameter used to reflect the spatial structure of an object. It can reflect the aggregation mechanism in an all-round way. The  $D_f$  of aggregates is generally calculated by the following formula:

$$N = k_f \left( \frac{2R_g}{d_p} \right)^{D_f} \quad (3-1)$$

$d_p$  is the average diameter of the elementary particle,  $k_f$  is the front factor,  $R_g$  is the radius of gyration of the aggregates, and  $n$  is the number of elementary particle, which can be calculated by Formula 2:

$$N = k_\alpha \left( \frac{A_\alpha}{A_p} \right)^\alpha \quad (3-2)$$

In the formula,  $A_\alpha$  is the projection area of the aggregates, which can be measured directly in the image processing software.  $A_p$  is the average projection area of the aggregates calculated by  $d_p$ , and  $k_\alpha$  and  $\alpha$  are the empirical parameters. Brasil also believes that there is an approximate relationship between  $R_g$  and  $L$  (3-3).

$$L/(2R_g) = 1.50 \pm 0.05 \quad (3-3)$$

The final formula for calculating the fractal dimension is shown in Formula 4. For a more detailed explanation, please refer to the Brasil et al. [17] method and the references cited therein.

$$N = k_{fL} \left( L/d_p \right)^{D_f} \quad (3-4)$$

$k_{fL}$  is a pre-correlation factor term similar to  $k_f$ , which determines the size of the least square linear fitting curve between  $N$  and  $L/d_p$ .

In the present study, the  $D_f$  and the  $D_g$  of the aggregates were taken into account when quantifying the morphological differences of the elementary particle aggregates. This parameter reflects the size of aggregates, from which we can get some information about the formation of aggregates. According to the previous research, based on the  $D_f$ , the  $D_g$  of aggregates can be calculated:

$$D_g/L = (D_f/(D_f + 2))^{1/2} \quad (3-5)$$

Figure 5 shows the statistical results of the  $D_f$  of particulate elementary particle aggregates at 25% engine load when diesel fuel with different sulfur contents is burned at S0.005, S0.05 and S0.26. The linear data were fitted according to the scatter values from several TEM images, the Pearson's R values in figure 5 (a), (b) and (c) are 0.942, 0.938 and 0.908, respectively. As the sulfur content of the fuel increases, the  $D_f$  of the aggregates increases, from 1.281 to 1.553. The large  $D_f$  indicates that the aggregate structure is dominated by cluster-like elementary particle, and the overlap between the basic carbon particles is large. As shown in Fig. 6, with the increase of FSC, the overall shape of the particles gradually changes from a clear chain structure to a cluster structure with an obscure boundary. The results show that the particle aggregates formed at high FSC are more compact and the particle aggregates formed at low sulfur content are relatively loose. For the basic carbon particles of particulate matter produced by fuel with high sulfur content, the aggregate structure is more compact, which will lead to the increase of FSN of emission particles.

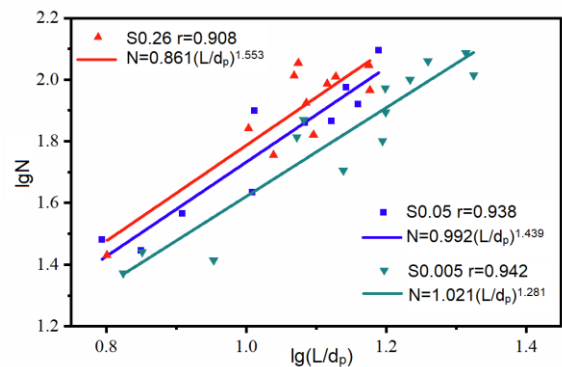


Fig 5. Statistical Determination of  $D_f$  of particulate aggregates with different FSC (a) S0.005, (b) S0.05, (c) S0.26

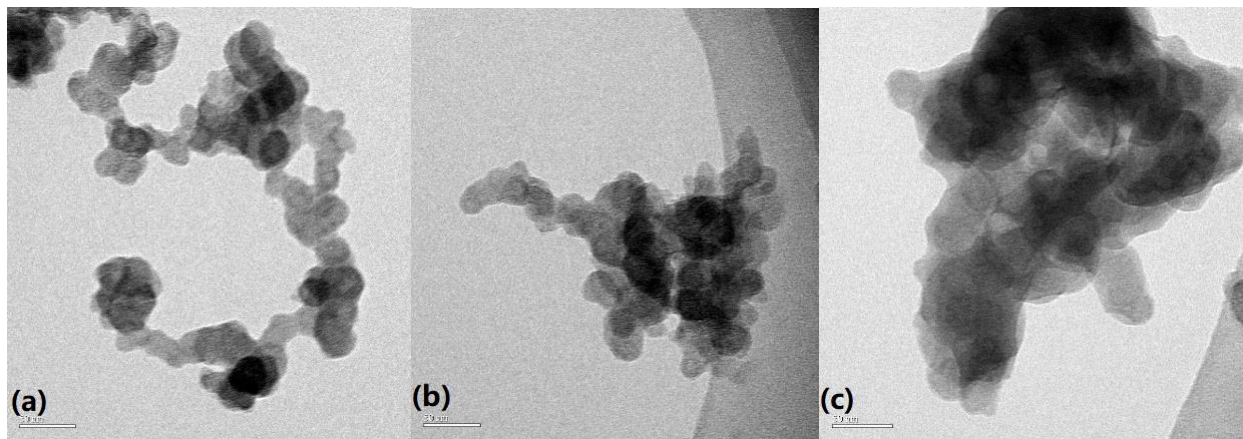


Fig. 6 Micro-morphology of particulate matter with different FSC (a) S0.005, (b) S0.05, (c) S0.26

The diameter distribution of the aggregates is shown in Figure 7. The statistical results show that the  $D_g$  of all aggregates are in the range of 50 ~ 300nm, which is consistent with the results of other studies. It can be observed intuitively in the diagram that the distribution of the diameter of gyration of agglomerates shifts to a larger size range with the increase of sulfur content in the fuel. More specifically, 69.23% of the aggregates obtained with S0.005 fuel had a  $D_g$  of less than 200 nm, and as the sulfur content in the fuel increased, in the case of S0.26, the ratio was reduced to 36.36%. The same trend was also found when comparing the average diameter of particle aggregates of three fuels with different sulfur contents. The average diameter of particle aggregates increased from 164.58 nm at S0.005 to 214.44 nm at S0.26. Thus, an increase in FSC increases the size of the aggregate particles produced by combustion. The particles released by burning sulfur-containing fuel contain organic components and sulfates, and the increase in sulfates contributes to the formation of larger particles, which increase the probability of particle collisions, and because the surface of the high sulfur particles agglomerates and adsorbs more organic components, the metal ash content is also more, its Van der Waals force, adsorption force, electrostatic force and other intermolecular force are also greater [18], similar particles tend to stick together when they collide, so many of them coalesce into a mass that causes a decrease in PN.

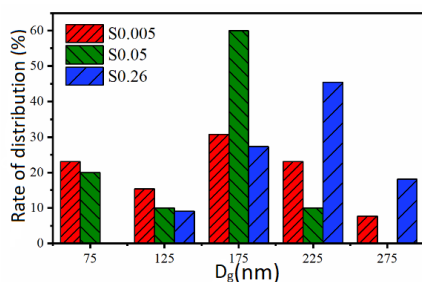


Figure 7. Size distribution of diesel particulate matter aggregates with different FSC

To sum up, the  $D_f$  and  $D_g$  of particulate matter increase with the increase of FSC, and with the increase of  $D_f$ , the structure of particulate aggregates becomes more compact, which leads to the increase of FSN of particulate matter, however, the increase of the diameter of gyration is due to the adsorption and incorporation of more particles by the aggregates, which results in the decrease of the number of PN and the increase of FSN, FSC has the opposite effect on FSN and PN, this results in differences in the FSN and PN of particulate matter.

#### 4. CONCLUSION

The effects of engine load, FSC on engine performance, emissions and particulate matter properties were studied on a marine auxiliary engine. The conclusions are summarized as follows:

(1) BTE decreases with the increase of FSC. The sulfur element in the fuel will react with oxygen during the combustion process, which will affect the combustion in the cylinder.

(2) The incomplete combustion products and the intermediate products produced by the pyrolysis of macromolecular fuels are mainly concentrated in the regions with high sulfur content and low engine load. The products of complete combustion are mainly located in the high load condition of the engine, and the particulate matter and  $SO_2$  emissions are distributed in the region with high sulfur content. Sulfur in fuel can promote the formation of incomplete combustion products and intermediate products during combustion, possibly by promoting the fracture of carbon-carbon bond.

(3) With the increase of FSC, the  $D_f$  and  $D_g$  of particle aggregates increase, particle aggregates are made up of more particles and have a denser structure, the FSN of particulate matter increases and the PN decreases,

which leads to the emission trends of FSN and PN were not consistent.

#### DECLARATION OF INTEREST STATEMENT

The authors declare that they have no known competing financial interests or personal relationships that could have appeared to influence the work reported in this paper.

#### ACKNOWLEDGMENTS

This work was supported by the National Natural Science Foundation of China (No. 51976135, No. 21961122007, and No. 51806148).

#### REFERENCES

[1] Eyring V, Isaksen I, Berntsen T, Collons W, Corbett J, Endresen O, Grainger R, Moldanova J, Schlager H, Stevenson D. Transport impacts on atmosphere and climate: Shipping. *Atmos. Environ.* 2010;44:4735–71.

[2] IMO. Third IMO greenhouse gas study. International Maritime Organization 2014.

[3] MARPOL 73/78: Annex VI. Regulations for the prevention of air pollution from ships and NO<sub>x</sub> technical code.

[4] Wang H, Yao A, Yao C, Wang B, Wu T, Chen C. Investigation to meet China II emission legislation for marine diesel engine with diesel methanol compound combustion technology. *J. Environ. Sci.* 2020;96:99–108.

[5] Ni P, Wang X, Li H. A review on regulations, current status, effects and reduction strategies of emissions for marine diesel engines. *Fuel* 2020;279:118477.

[6] TAN P, HU Z, LOU D. Regulated and unregulated emissions from a light-duty diesel engine with different sulfur content fuels [J]. *Fuel*, 2009, 88: 1086–1091.

[7] TAN P, LI Y, SHEN H. Effect of Lubricant Sulfur on the Morphology and Elemental Composition of Diesel Exhaust Particles[J]. *Journal of Environmental Sciences*, 2017, 55: 354–362. DOI:10.1016/j.jes.2017.01.014.

[8] VAN T, RISTOVSKI Z, SURAWSKI N, BODISCO T, RAHMAN S, ALROE J, MILJEVIC B, HOSSAIN F, SUARA K, RAINEY T, BROWN R. Effect of sulphur and vanadium spiked fuels on particle characteristics and engine performance of auxiliary diesel engines [J]. *Environmental Pollution*, 2018, 243: 1943-1951.

[9] ZHAO Y, MA Q, LIU Y, Influence of Sulfur in Fuel on the Properties of Diffusion Flame Soot[J]. *Atmospheric Environment*, 2016, 142: 383 – 392.

[10] GENG P, TAN Q, ZHANG C, WEI L, HE X, CAO E, JIANG K. Experimental investigation on NO<sub>x</sub> and green house gas emissions from a marine auxiliary diesel engine using ultralow sulfur light fuel [J]. *Science of the Total Environment*, 2016, 572: 467–475.

[11] VAN T, SURAWSKI N, RISTOVSKI Z, YUAN C, STEVANOVIC S, RAHMAN S, HOSSAIN F, GUO Y, RAINEY T, BROWN R. The effect of diesel fuel sulphur and vanadium on engine performance and emissions [J]. *Fuel*, 2020, 261: 116437.

[12] LAIK D, CORBETT J. Black carbon from ships: a review of the effects of ship speed, fuel quality and exhaust gas scrubbing [J]. *ATMOSPHERIC CHEMISTRY AND PHYSICS*, 2012, 12: 3985–4000.

[13] TAKADA K, YOSHIMURA F, OHGA Y, KUSAKA J, DAISHO Y. Experimental study on unregulated emission characteristics of turbocharged DI diesel engine with common rail fuel injection system. *SAE Technical Paper*, 2003, 2003-01-3158.

[14] SHEN W, BAI S, WANG K,. Simplified Modeling Combustion Chemistry of Neat and Blended Large Hydrocarbon Fuels with Different Functional Groups[J]. *Combustion and Flame*, 2021, 234: 111610. DOI:10.1016/j.combustflame.2021.111610.

[15] BRADY J, CRISP T, COLLIER S, KUWAYAMA T, FORESTIERI S, PERRAUD V. Realtime emission factor measurements of isocyanic acid from light duty gasoline vehicles [J]. *Environmental Science Technology*, 2014, 48:11405–11412.

[16] KUMAR V, SINGH A, AGARWAL A. Gaseous emissions (regulated and unregulated) and particulate characteristics of a medium-duty CRDI transportation diesel engine fueled with diesel-alcohol blends [J]. *Fuel*, 2020, 278: 118269.

[17] BRASIL A M, FARIAS T L, CARVALHO M G. A RECIPE FOR IMAGE CHARACTERIZATION OF FRACTAL-LIKE AGGREGATES [J]. *Journal of Aerosol Science*, 1999, 30(10): 1379-89.

[18] CHEN N, SONG C, LV G, et al. Atom force microscopy analysis of the morphology, attractive force, adhesive force and Young's modulus of diesel in-cylinder soot particles [J]. *COMBUSTION AND FLAME*, 2015, 162(12): 4649-59